Mechanistic insights into the water-catalysed ring-opening reaction of vitamin E by means of double-hybrid density functional theory

Farzaneh Sarrami, Asja A. Kroeger, Amir Karton*

School of Molecular Sciences, The University of Western Australia, Perth, WA 6009, Australia

The potent antioxidant α-tocopherol is known to trap two hydroxyl radicals leading to the formation of the experimentally observed α-tocopherylquinone product. Based on double-hybrid density functional theory calculations, we propose for the first time, a reaction mechanism for the conversion of α-tocopherol to α-tocopherylquinone. We find that a water-catalysed ring-opening reaction plays a key role in this conversion. The water catalysts act as proton shuttles facilitating the proton transfers and reducing the ring strain in the cyclic transition structures. On the basis of the proposed reaction mechanism, we proceed to design an antioxidant with potentially enhanced antioxidant properties.

Keywords: Density functional theory, Water catalysis, Vitamin E

*Corresponding author: amir.karton@uwa.edu.au

1. Introduction

Oxidative damage from reactive oxygen species such as the hydroxyl or hydroperoxyl radical to DNA, proteins, and lipids can lead to a broad range of chronic diseases such as Parkinson's and Alzheimer's disease.[1,2,3,4] Biological systems protect themselves from such oxidative damage with radical scavenging antioxidants, of which some are hydrophilic and some are lipophilic.[5,6,7] Vitamin E is an important lipid-soluble antioxidant occurring in lipoproteins and membranes.[8,9] It may exist in a number of different forms, each containing a chemically reactive heterocyclic chromane moiety that is responsible for antioxidant activity and an unreactive lipophilic alkyl side-chain.[10] The most active form of vitamin E, α-tocopherol (AT), is illustrated in Figure 1. Numerous studies on the biological activities of this antioxidant have found that it plays an important part in disease prevention. Research by Maydani showed that α-tocopherol may inhibit oxidation of low-density lipoprotein (LDL) cholesterol in plasma, thereby supporting the treatment of cardiovascular diseases.[11,12] It was further found to reduce cancer cell proliferation in breast cancers[13] and has shown anti-androgen activity in prostate carcinoma cells, making it a potent chemopreventive agent of androgen-dependent diseases.[14] These promising results have encouraged a wide range of experimental as well as theoretical studies investigating the antioxidant activity of **AT** aimed at gaining a better understanding on its mechanism of action.[15,16,17,18]

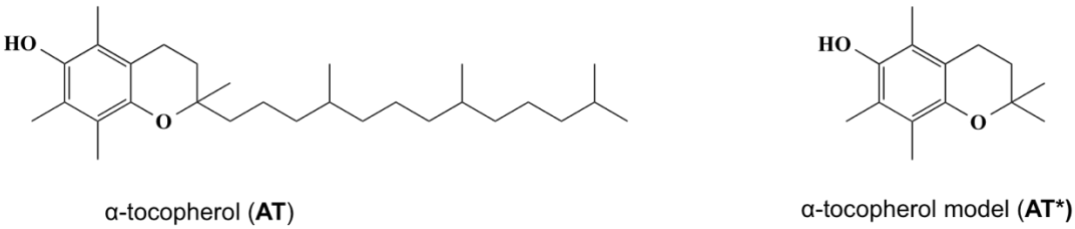

α-tocopherol (**AT**) α-tocopherol model (**AT***)

Figure 1. Structures of α-tocopherol (AT) and a model system investigated in the present study (AT*), in which the long alkyl chain has been replaced with a methyl group.

It was found that a single molecule of **AT** may trap two hydroxyl radicals leading to the major oxidation product α-tocopherylquinone (**ATQ**).[19] Figure 2 illustrates the proposed mechanism of this reaction. A hydrogen abstraction from the hydroxyl group by the first hydroxyl radical leads to the tocopheroxyl radical. Tocopheroxyl radicals are resonance-stabilised free radicals that are important intermediates in the antioxidant activity of vitamin E, since they may participate in radical-radical termination reactions. Addition of a second hydroxyl radical to the carbon neighboring the endocyclic oxygen and subsequent ring-opening lead to the α-tocopherylquinone (**ATQ**) product.

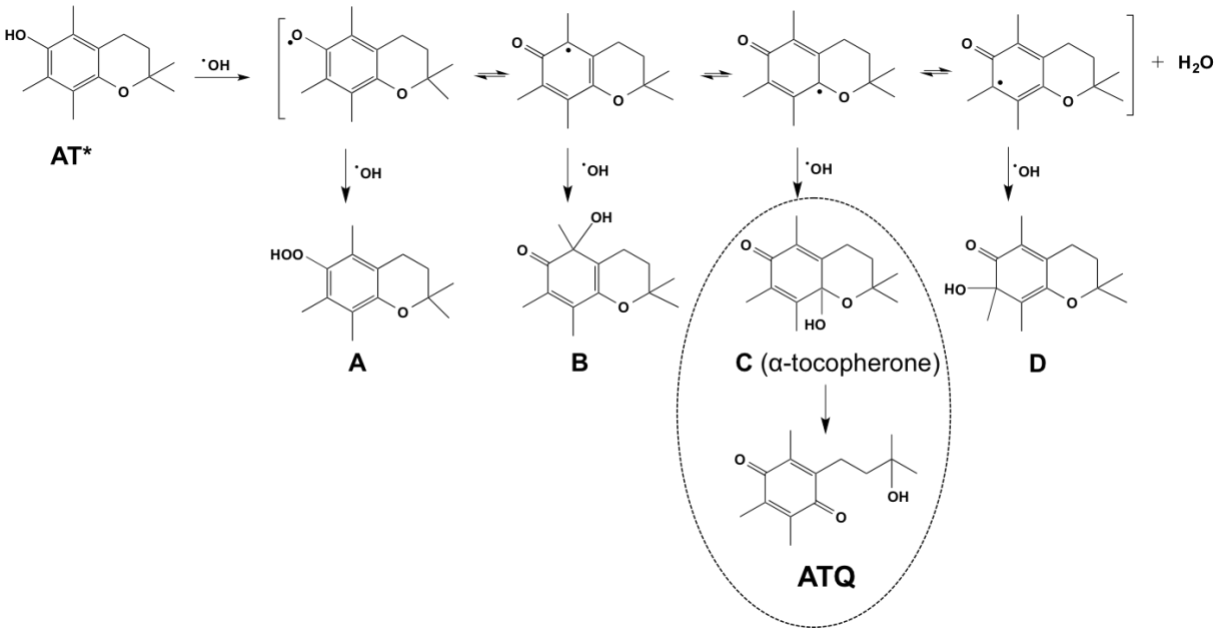

Figure 2. The reaction mechanism for the antioxidant activity of α-tocopherol (AT*), through the reaction with two hydroxyl radicals. The ring-opening reaction leading to ATQ is the subject of the present work and shown in a dashed circle.

A number of computational studies investigated the reaction of **AT** with a single hydroxyl or hydroperoxyl radical to give α-tocopherone.[20,21,22] Navarrete *et al.*[20] investigated the hydrogen abstraction from the phenolic hydrogen by hydroxyl and hydroperoxyl radicals.[21] Chen *et al.*[22] considered the bond dissociation energies associated with the first hydrogen abstraction of **AT** and structure function relationships in related structures. They showed that reducing the size of the heterocyclic ring is likely to give better antioxidant activity. Replacing the oxygen atom in **AT** with S or Se, on the other hand, appeared to reduce antioxidant activity. Wright *et al.* [23] investigated substituent effects on the O–H bond strength of phenolic antioxidants related to vitamin E. To the best of our knowledge, the mechanism of the second radical scavenging process leading to the final **ATQ** oxidation product has not been studied computationally. Here we use high-level double-hybrid DFT methods to investigate the reaction pathway of the rearrangement of α-tocopherone to form **ATQ**. We consider both the uncatalysed and water-catalysed reaction pathways. Based on our proposed

reaction mechanism, we proceed to design vitamin E-related antioxidants with improved antioxidant properties.

2. Computational details

The geometries of all structures were optimized using the B3LYP-D3 density functional theory (DFT) exchange-correlation functional in conjunction with the 6-31G(2df,p) Pople-style basis set.[24,25,26] Empirical D3 dispersion corrections[27] were included using the Becke−Johnson[28] damping potential as recommended in ref. 26 (denoted by the suffix-D3). Bulk solvent effects in aqueous solution were included using the charge-density-based CPCM polarizable solvation model.[29] Harmonic vibrational analyses have been performed at the same level of theory to confirm each stationary point as either an equilibrium structure (i.e., all real frequencies) or a transition structure (i.e., with one imaginary frequency). Zero-point vibrational energies and thermal correction to the enthalpy have been obtained from these calculations. We note that the main text primarily looks at ΔH_{298} values to allow a discussion of the energetic effects in the uncatalysed and catalysed reaction mechanisms, however, similar trends are observed on the Gibbs free energy (ΔG_{298}) reaction profiles, which are given in Figures S1–S3 and Table S1 of the Supporting Information. The connectivity of the local minima and first-order saddle points was confirmed by performing intrinsic reaction coordinate calculations.[30] High-level DHDFT calculations using the spin-component-scaled DSD-PBEP86-D3 functional were performed in order to obtain accurate electronic energies for the equilibrium and transition structures located along the uncatalysed and catalysed reaction pathways.[31] These DHDFT procedures involve second-order Møller–Plesset perturbation theory to overcome limitations of traditional DFT methods and display excellent performance for challenging chemical problems.[32,33,34,35,36] DHDFT has been found to produce thermochemical properties (such as reaction energies and barrier heights) with mean

absolute deviations (MADs) approaching the threshold of 'chemical accuracy' (arbitrarily defined as 4.2 kJ mol^{-1}). The DHDFT calculations, which inherit the slow basis-set convergence of MP2, are carried out with the quadruple-zeta Def2-QZVPP basis set.[37] Corrections for bulk solvent effects in aqueous solution were added to the gas-phase DHDFT energies using the CPCM model at the HF/6-31+G(d) level of theory as recommended in ref. 38 The resulting level of theory is denoted by CPCM(water)-DSD-PBEP86. The Gaussian16 suite of programs was used for all the DFT and DHDFT calculations.[39]

3. Results and discussion

We begin by considering the possible reactions of the tocopheroxyl radical with the hydroxyl radical. Figure 2 shows the four resonance structures of the tocopheroxyl radical along with the four possible products of the radical coupling reaction (denoted **A**, **B**, **C**, and **D)**. Table 1 gives the reaction enthalpies for these four species relative to the free reactant (**AT***). As expected, intermediates **B**, **C**, and **D** are vastly favoured over intermediate **A**, which contains a reactive peroxide group. Intermediate **C**, the only structure that can undergo rearrangement to **ATQ**, is thermodynamically more stable than intermediates **B** and **D** by 21.2–21.8 kJ mol^{-1}. We note that similar trends are observed on the ΔG_{298} potential energy surface (for further details see Table S1). In the following sections we will consider the uncatalysed and water-catalysed rearrangement reactions for the formation of **ATQ** from intermediate **C**.

Table 1. Reaction enthalpies (ΔH_{298}) calculated at the CPCM(water)-DSD-PBEP86 level for the four possible products (**A**, **B**, **C**, and **D**) of the radical coupling reaction between the tocopheroxyl radical and HO• (Figure 2). Enthalpies in kJ mol^{-1} are given relative to the free reactants.

Intermediate	ΔH_{298}
A	–114.2
B	–281.3
C	–302.5
D	–280.7

3.1. Rearrangement reaction of α-tocopherone to quinone

3.1.1. Uncatalysed reaction mechanism

The reaction profile for the uncatalysed ring-opening of α-tocopherone is given in Figure 3. The reaction mechanism involves a proton transfer from O^1 to O^2, concomitant with the breaking of the C^1–O^2 bond and the formation of a double bond between C^1 and O^1. This concerted ring-opening reaction is associated with a fairly high activation enthalpy of 159.9 kJ mol^{-1}, which is largely attributed to the highly strained four-membered cyclic transition structure. The **ATQ** product lies 7.1 kJ mol^{-1} below α-tocopherone. We note that on the ΔG_{298} potential energy surface the reaction is exergonic by 16.7 kJ mol^{-1} and the activation Gibbs free energy is 158.9 kJ mol^{-1} (for further details see Figure S1).

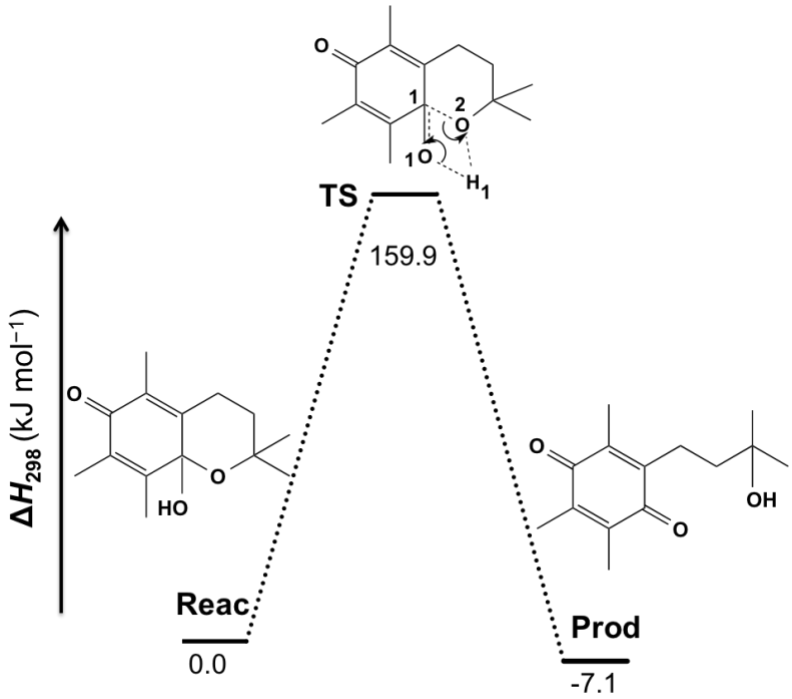

Figure 3. Reaction profile (ΔH_{298}, CPCM(water)-DSD-PBEP86, kJ mol^{-1}) for the uncatalysed rearrangement reaction of α-tocopherone to **ATQ**. The bonds being broken and formed in the transition structures are represented by black dashed lines.

3.1.2. Water-catalysed reaction mechanism

The participation of catalytic water molecules in reactions involving proton transfers is well documented and can significantly reduce activation barriers by reducing strain energies involved in the TSs.[40,41,42,43,44,45,46] Here, we examine the catalytic effect of one and two explicit water molecules on the rearrangement reaction of α-tocopherone to **ATQ**. The reaction profile for the H_2O-catalysed reaction is shown in Figure 4 (red line). In the reactant complex (**RC**), the water molecule is hydrogen bonded to the hydroxyl group of the tocopherone via one hydrogen bond (1.806 Å). As a result, the reactant complex is more stable than the free reactants by 25.5 kJ mol^{-1}. Participation of water in the transition structure reduces the activation enthalpy of the rearrangement by 58.1 kJ mol^{-1}, from 159.9 (uncatalysed) to 101.8 (H_2O-catalysed) kJ mol^{-1} by expanding the transition structure from a four-membered ring TS to a less strained six-membered ring TS. We note that the activation energy for the catalysed reaction is 127.3 kJ mol^{-1} relative to the **RC**. The product complex

(**PC**) is stabilised by two hydrogen bonds, one between water and quinone (1.859 Å) and a longer hydrogen bond (1.915 Å) between the newly formed hydroxyl group and water (Figure 4). As a result the **PC** is 32.6 kJ mol^{-1} more stable than the free reactants.

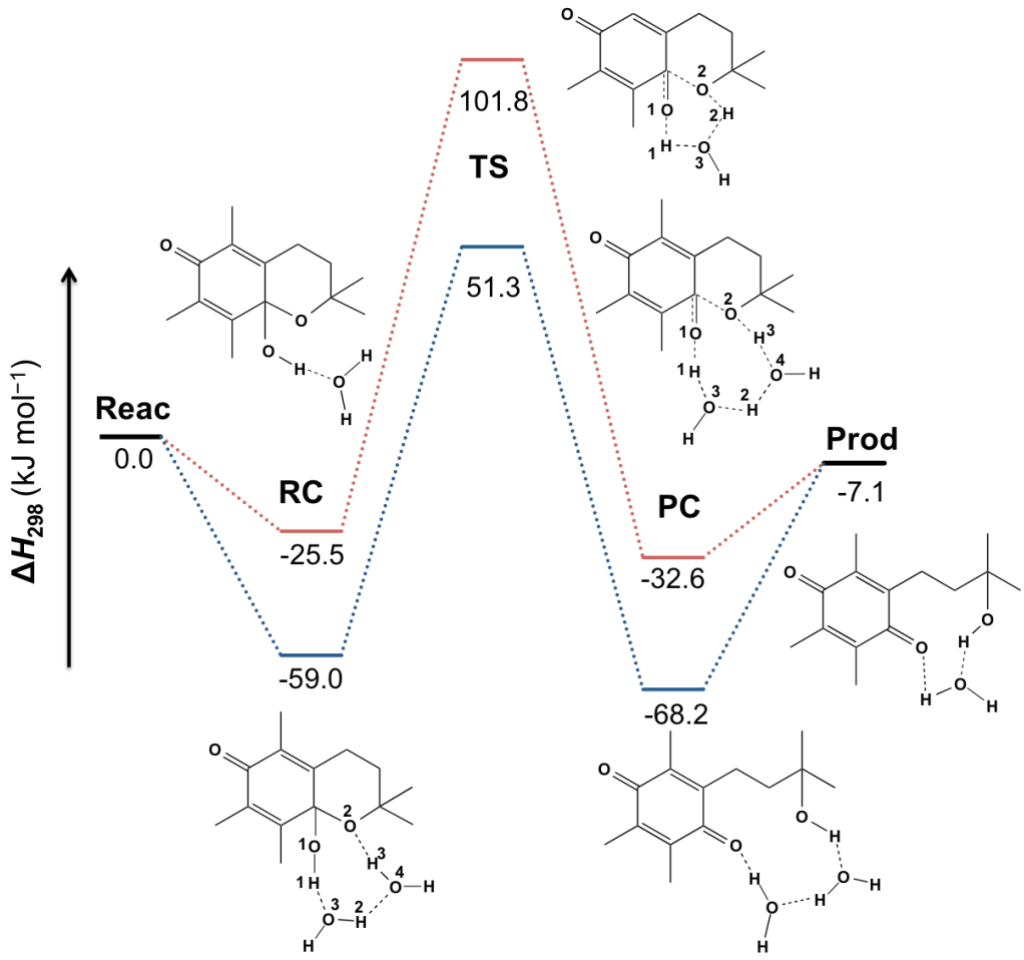

Figure 4. Reaction profile (ΔH_{298}, CPCM(water)-DSD-PBEP86, kJ mol^{-1}) for the rearrangement reaction of α-tocopherone to **ATQ** catalysed by one (red line) and two (blue line) water molecules. Dashed lines in the transition structures represent bonds being broken and formed, whilst in the RCs and PCs dashed lines represent hydrogen bonds.

The inclusion of two explicit water molecules expands the hydrogen bond network facilitating the proton transfer. As illustrated in Figure 4, in the **RC** the two water molecules form a bridge between the exocyclic hydroxyl group and the oxygen of the chromane moiety via three hydrogen bonding interactions. The lengths of these hydrogen bonds are 1.781

(H^1•••O^3), 1.781 (H^2•••O^4), and 1.916 (H^3•••O^2) Å (Figure 4). Accordingly, the **RC** lies 59.0 kJ mol^{-1} below the energy of the free reactants. In the subsequent transition structure the two water molecules act as proton shuttles, facilitating the proton transfer via an eight-membered cyclic TS. The TS lies 110.3 kJ mol^{-1} above the **RC**. Thus, compared to the uncatalysed pathway, participation of two water molecules decreases the activation energy towards the rearrangement by as much as 49.6 kJ mol^{-1}. Similarly to the **RC**, the **PC** formed between the product and the two water catalysts involves three strong hydrogen bonds (1.790 (H^1•••O^1), 1.750 (H^2•••O^3), and 1.786 (H^3•••O^4) Å, Figure 4) and lies 68.2 kJ mol^{-1} below the energy of the free reactants. Finally, we note that on the Gibbs free energy surface similar reaction barriers are obtained for the reactions catalysed by one and two water molecules (Figure S2 of the Supporting Information). This is consistent with previous results for water-catalysed proton transfers, which show that on the ΔG_{298} surface the most significant reduction in the barrier height is provided by the first water catalyst and inclusion of a second water catalyst has a minor effect.[33]

Further inspection of the transition structures of the catalysed and uncatalysed pathways, as depicted in Figure 5, indicates significant changes in geometries upon catalysis. Most notably, the inclusion of explicit catalytic water molecules improves the trajectories of the proton transfers. While the transition structure of the uncatalysed reaction leads to a highly unfavourable angle of $\angle O^1\text{-}H^1\text{-}O^2 = 125.6°$ for the first proton transfer, this improves to 158.0° ($\angle O^1\text{-}H^1\text{-}O^3$) and 161.0° ($\angle O^3\text{-}H^2\text{-}O^2$) in the H_2O-catalysed pathway. Near-ideal angles of 171.8° ($\angle O^1\text{-}H^1\text{-}O^2$), 165.3° ($\angle O^4\text{-}H^3\text{-}O^2$), and 176.6° ($\angle O^6\text{-}H^7\text{-}O^8$) are observed in the $2H_2O$-catalysed pathway. It is well known that in reactions at the carbonyl group an ideal angle of the incoming or leaving substituent relative to the carbonyl improves the stabilising overlap of the highest occupied molecular orbital (HOMO) of the nucleophile and the unoccupied carbonyl π^* orbital while minimizing steric interactions. Deviation from the ideal

trajectory of ~107–110°, leads to a rapid increase in activation energies.[47] While in the transition structure of the uncatalysed pathway this trajectory is highly unfavourable with an angle of $\angle O^2\text{-}C^1\text{-}O^1$ = 89.3°, participation of the water catalysts allows for this angle to increase to $\angle O^2\text{-}C^1\text{-}O^1$ = 103.3° (1 H_2O catalyst) and $\angle O^2\text{-}C^1\text{-}O^1$ = 111.0° (2 H_2O catalysts). Further, it is instructive to note that the opening six-membered heterocyclic ring assumes favourable chair-conformations in the transition structures of the water-catalysed pathways, whereas a twisted boat-like geometry is observed for the uncatalysed pathway.

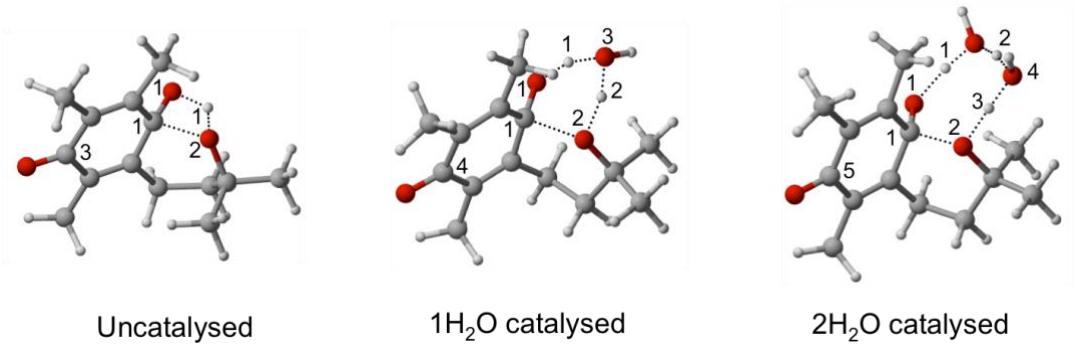

Figure 5. Transition structures for the uncatalysed, 1H_2O-catalysed, and 2H_2O-catalysed rearrangement reaction of α-tocopherone to **ATQ**. The bonds being broken and formed in the transition structures are represented by black dashed lines.

3.2. Rational design of vitamin E based antioxidants

It is well known that the presence of a saturated heterocycle is essential for the antioxidant activity of chromanols.[48] Several previous studies aimed at designing novel antioxidants have found that changes to the atom number of the heterocyclic ring as well as substituting the heteroatom of the chromanol moiety affect antioxidant activity with regard to the first radical scavenging reaction. There is general agreement in the literature that reducing the number of atoms in the heterocyclic ring has the potential to improve antioxidant activity.[22,49,50] In order to test if a similar trend can be observed for the scavenging of a second hydroxyl radical, derivatives of α-tocopherol with a modified heterocyclic ring are considered in this work and depicted in Scheme 1.

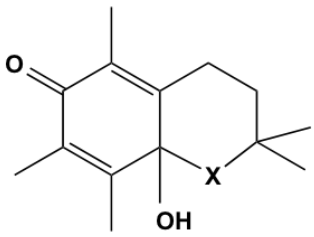

X = O	heterocyclic ring (6)	α-tocopherone
X = O	heterocyclic ring (4)	Candidate 1
X = O	heterocyclic ring (5)	Candidate 2
X = S	heterocyclic ring (6)	Candidate 3

Scheme 1. Structures of the α-tocopherol derivatives investigated in this work. The number in brackets indicates to the number of atoms in the heterocyclic.

We begin with examining the effect of the size of the heterocyclic ring in order to reduce the reaction barrier for the intramolecular ring-opening step. Figure 6 shows the enthalpic energy surfaces for the rearrangements of candidate 1. The reaction barrier height for the uncatalysed ring-opening reaction ($\Delta H_{298}^{\ddagger}$ = 124.4 kJ mol^{-1}) is lower by 35.9 kJ mol^{-1} compared to α-tocopherone ($\Delta H_{298}^{\ddagger}$ = 159.9 kJ mol^{-1}, Figure 3). This may be attributed to the fact that there is a larger reduction in ring strain upon rearrangement when going from a 6-membered to a 4-membered ring. Further inspection of the geometries of the transition structures of the uncatalysed rearrangement of α-tocopherone and candidate 1, as illustrated in Figure 7, reveals increasing bond lengths of the forming H–O bond between the transferring proton and the oxygen atom of the opening heterocycle. Whereas in the transition structure pertaining to α-tocopherone a bond length of 1.217 Å is observed, this bond is increased to 1.783 Å in candidate 1. Thus, a four-membered heterocyclic ring leads to a transition structure that is earlier in the proton transfer and therefore of lower energy. The same trend is seen for the H–O bond being broken, namely it is significantly shorter in the TS with the four-membered ring (0.989 Å) than in the TS with the six-membered ring (1.249 Å).

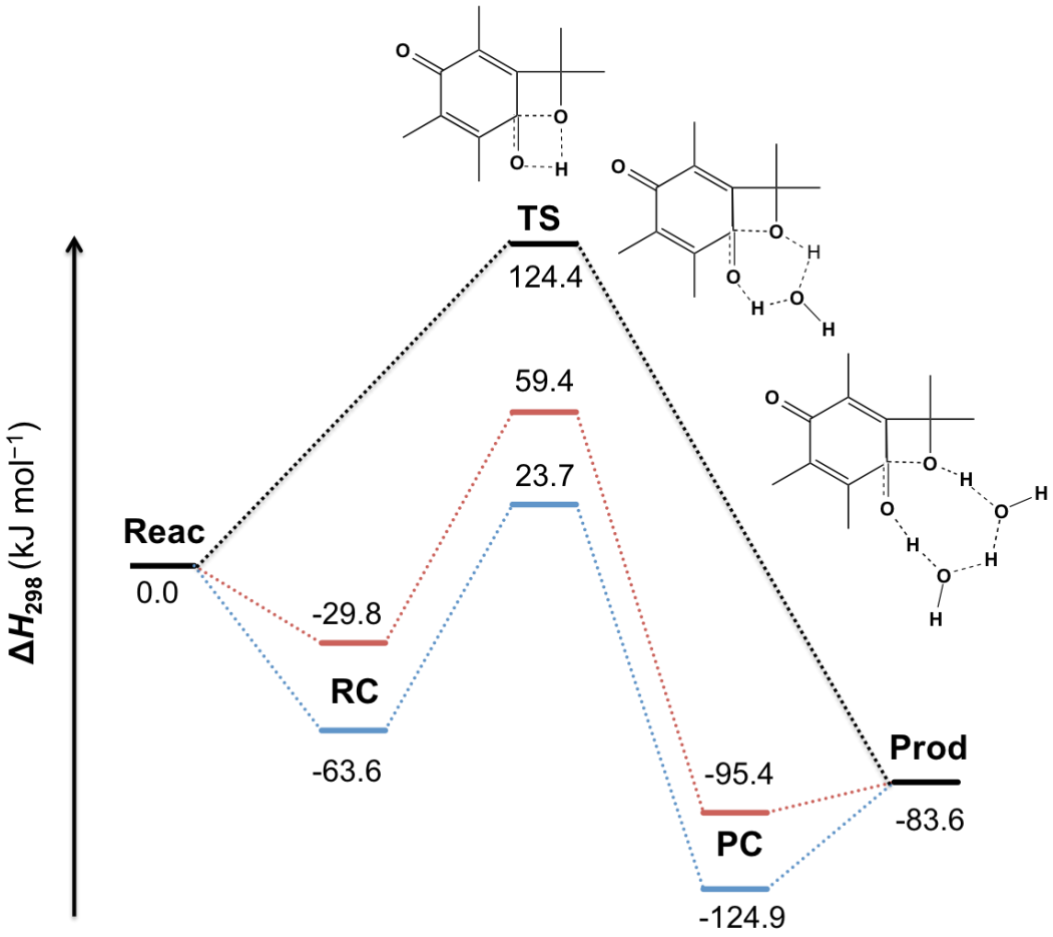

Figure 6. Reaction profile (ΔH_{298}, CPCM(water)-DSD-PBEP86, kJ mol^{-1}) for the uncatalysed (black line), H_2O-catalysed (red line), and $2H_2O$-catalysed (blue line) rearrangement reaction in the proposed antioxidant candidate 1 (Scheme 1). A schematic representation of the TSs is shown in which bonds being broken and formed are represented by dashed lines.

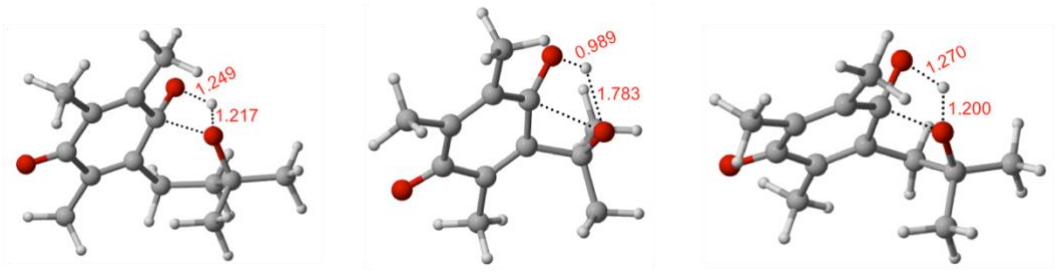

Figure 7. Optimised transition structures obtained for the ring-opening reaction of α-tocopherone and the two potential antioxidant candidates considered in present work. The bonds being broken and formed in the transition structures are represented by black dashed lines.

Figure 6 gives the reaction profile for the H_2O-catalysed (red line) and $2H_2O$-catalysed (blue line) rearrangements of candidate 1. Similar to the findings presented in section 3.1, participation of catalytic water molecules as proton shuttles reduces the energy barriers towards ring-opening. In particular, the barrier height for the H_2O-catalysed reaction is reduced from 127.3 (α-tocopherone) to 89.4 (candidate 1) kJ mol^{-1}, note that these reaction barrier heights are taken relative to the RCs (Figures 4 and 6). The reduction in the barrier height is less pronounced for the reaction catalysed by two water molecules. Namely, the barrier heights are 110.3 (α-tocopherone) and 87.3 (candidate 1) kJ mol^{-1}. We note that similar results are obtained on the Gibbs free energy surface, that is inclusion of a second water catalyst does not provide further catalytic enhancement (see Figure S3 of the Supporting Information).

An important aspect in the improved antioxidant activity of candidate 1 is that it provides a strong thermodynamic driving force for the overall reaction. The ring-opening reaction is exothermic by 83.6 (uncatalysed) and 65.6 (1 H_2O catalyst), and 61.3 (2 H_2O catalysts) kJ mol^{-1} (Figure 6). These reaction enthalpies should be compared to reaction enthalpies of merely 7–9 kJ mol^{-1} obtained for the uncatalysed and catalysed ring-opening reactions in α-tocopherone (Figures 3 and 4).

Figures S4 and S5 of the Supporting Information give the reaction profiles for the uncatalysed, H_2O-catalysed, and $2H_2O$-catalysed rearrangements for candidates 2 and 3 (Scheme 1). These candidates, however, do not lead to a significant improvement over α-tocopherone in either the reaction barrier height or in the thermodynamic driving force for the reaction.

Conclusions

The antioxidant α-tocopherol (a.k.a. vitamin E) is known to react with two OH radicals to form α-tocopherylquinone. The first reaction with OH is a hydrogen-abstraction reaction which forms a tocopheroxyl radical. This reaction has been the subject of theoretical investigations. However, the subsequent reaction leading to the formation of α-tocopherylquinone has not been studied computationally. On the basis of DHDFT computational modelling, we propose a mechanism for the intramolecular ring-opening reaction of α-tocopherone leading to the final α-tocopherylquinone. We find that the uncatalysed intramolecular ring-opening reaction proceeds via a strained four-membered transition structure. Accordingly, this reaction is associated with a high activation enthalpy of 159.9 kJ mol^{-1}. Involvement of one and two water catalysts in the TS reduce the reaction barrier height to 127.3 and 110.3 kJ mol^{-1}, respectively. This catalytic efficiency can be rationalised by (i) the reduction in strain energy in the TSs in the order uncatalysed, 1 H_2O catalyst, and 2 H_2O catalysts, and (ii) improved trajectories for the proton transfers from the hydroxyl group to the heterocyclic oxygen.

We find that the proposed reaction mechanism also applies to structurally-related systems in which the size of the heterocyclic ring is reduced and the heterocyclic oxygen is replaced with a sulfur atom. Our results show that reducing the size of the heterocyclic ring of the α-tocopherone to a four-membered ring not only reduces the barrier for the ring-opening reaction but also significantly increases the thermodynamic driving force for the overall reaction. In particular, for the four-membered-ring analogue of α-tocopherol we obtain reaction barrier heights of 89.2 and 87.3 kJ mol^{-1} for the reactions catalysed by one and two water molecules, respectively (cf. with reaction barriers of 127.3 and 110.3 kJ mol^{-1} for α-tocopherol). Importantly, the reaction with α-tocopherol is exothermic by merely 7.1–

9.2 kJ mol^{-1} (for the uncatalysed and catalysed reactions), however, for the four-membered-ring analogue the reaction is exothermic by 61.3–83.6 kJ mol^{-1} (for the uncatalysed and catalysed reactions). The significant reduction in the reaction barrier height and increase in the reaction exothermicity suggest that the four-membered-ring analogue of α-tocopherol could be a more efficient antioxidant than vitamin E for neutralising two equivalents of OH radicals.

Acknowledgments

This research was undertaken with the assistance of resources from the National Computational Infrastructure (NCI), which is supported by the Australian Government. We also acknowledge the system administration support provided by the Faculty of Science at the University of Western Australia to the Linux cluster of the Karton group. We gratefully acknowledge the provision of an Australian Postgraduate Award (to F.S.), a Forrest Research Foundation Scholarship and an Australian Government Research Training Program Stipend (to A.A.K.), and an Australian Research Council (ARC) Future Fellowship (to A.K.; Project No. FT170100373).

Supplementary data

CPCM(water)-DSD-PBEP86 Gibbs free energy (ΔG_{298}) reaction profiles for the reactions shown in Figure 3 (Figure S1), Figure 4 (Figure S2), and Figure 6 (Figure S3); Reaction profiles (ΔH_{298}, CPCM(water)-DSD-PBEP86) for the uncatalysed, H_2O-catalysed, and $2H_2O$-catalysed rearrangement reactions of candidate 2 (Figure S4) and candidate 3 (Figure S5) to the related quinones; CPCM(water)-DSD-PBEP86 ΔG_{298} values for the four possible products (**A**, **B**, **C**, and **D**) in Figure 2 (Table S1); CPCM(water)-B3LYP/6-31G(2df,p) optimised geometries for all the species considered in the present work (Tables S2 and S3).

References

[1] J. Vina, C. Borras, K. Mohamed, R. Garcia-Valles, M.C. Gomez-Cabrera. The free radical theory of aging revisited: the cell signaling disruption theory of aging. *Antioxid. Redox Signal* 19 (2013) 779.

[2] B. Uttara, A. V. Singh, P. Zamboni, R. T. Mahajan. Oxidative stress and neurodegenerative diseases: a review of upstream and downstream antioxidant therapeutic options. *Curr. Neuropharmacol* 7 (2009) 65.

[3] E. Mocchegiani, L. Costarelli, R. Giacconi, M. Malavolta, A. Basso, F. Piacenza, R. Ostan, E. Cevenini, E. S., Gonos, C. Franceschi, D. Monti. Vitamin E-gene interactions in aging and inflammatory age-related diseases: implications for treatment. A systematic review. *Ageing Res. Rev.* (2014) 81.

[4] M. Maes, P. Galecki, Y. S. Chang, M. Berk. A review on the oxidative and nitrosative stress (O&NS) pathways in major depression and their possible contribution to the (neuro)degenerative processes in that illness. *Prog. Neuropsychopharmacol. Biol. Psychiatry.* 35 (2011) 676.

[5] T. Yamamori, H. Yasui, M. Yamazumi, Y. Wada, Y. Nakamura, H. Nakamura, O. Inanami. Ionizing radiation induces mitochondrial reactive oxygen species production accompanied by upregulation of mitochondrial electron transport chain function and mitochondrial content under control of the cell cycle checkpoint. *Free Radic. Biol. Med.* 53 (2012) 260.

[6] H. Tominaga, S. Kodama, N. Matsuda, K. Suzuki, M. Watanabe. Involvement of reactive oxygen species (ROS) in the induction of genetic instability by radiation. *J. Radiat. Res.* 45 (2004) 181.

[7] E. Niki, N. Noguchi. Dynamics of antioxidant action of vitamin E. *Acc. Chem. Res.* 37 (2004) 45.

[8] G. W. Burton, K. U. Ingold. Vitamin E: application of the principles of physical organic chemistry to the exploration of its structure and function. *Acc. Chem. Res.* 19 (1986) 194.

[9] Q. Jiang. Natural forms of vitamin E: metabolism, antioxidant, and anti-inflammatory activities and their role in disease prevention and therapy. *Free Radic. Biol. Med.* 72 (2014) 76.

[10] E. Niki, A. Kawakami, M. Saito, Y. Yamamoto, J. Tsuchiya, Y. Kamiya. Effect of phytyl side chain of vitamin E on its antioxidant activity. *J. Biol. Chem.* 260 (1985) 2191.

[11] M. Maydani. Vitamin E. *The Lancet* 345 (1995) 170.

[12] A. P. Levy, S. Blum. Pharmacogenomics in prevention of diabetic cardiovascular disease: utilization of the haptoglobin genotype in determining benefit from vitamin E. *Expert Rev. Cardiovasc. Ther*. 5 (2007) 1105.

[13] N. Guthrie, A. Gapor, A. F. Chambers, K. K. Carroll. Inhibition of proliferation of estrogen receptor-negative MDA-MB-435 and -positive MCF-7 human breast cancer cells by palm oil tocotrienols and tamoxifen, alone and in combination. *J. Nutr*. 127 (1997) 544S.

[14] T. A. Thompson, G. Wilding. Androgen Antagonist Activity by the Antioxidant Moiety of Vitamin E, 2,2,5,7,8-Pentamethyl-6-chromanol in Human Prostate Carcinoma Cells. *Mol. Cancer Ther*. 2 (2003) 797.

[15] R. Loganathan, A. K. Radhakrishnan, K. R. Selvaduray, K. Nesaretnam. Selective anti-cancer effects of palm phytonutrients on human breast cancer cells. *RSC Adv.* 5 (2015) 1745.

[16] E. Niki, N. Noguchi. Dynamics of antioxidant action of vitamin E. *Acc. Chem. Res.* 37 (2004) 45.

[17] G. Mourente, E. Dıaz-Salvago, J. G. Bell, D. R. Tocher. Increased activities of hepatic antioxidant defence enzymes in juvenile gilthead sea bream (Sparus aurata L.) fed dietary oxidised oil: attenuation by dietary vitamin E. *Aquaculture* 214 (2002) 343.

[18] B. Turan, N. L. Acan, N. N. Ulusu, E. F.Tezcan. A comparative study on effect of dietary selenium and vitamin E on some antioxidant enzyme activities of liver and brain tissues. *Biol. Trace. Elem. Res.* 81 (2001) 141.

[19] R. Yamauchi. Vitamin E: Mechanism of Its Antioxidant Activity. *Food Sci. Technol. Int. Tokyo.* 3 (1997) 301.

[20] M. Navarrete, C. Rangel, J. C. Corchado, J. Espinosa-Garcia. Trapping of the OH radical by alpha-tocopherol: a theoretical study. *J. Phys. Chem. A.* 109 (2005) 4777.

[21] M. Navarrete, C. Rangel, J. Espinosa-Garcia, J. C. Corchado. Theoretical Study of the Antioxidant Activity of Vitamin E: Reactions of α-Tocopherol with the Hydroperoxy Radical. *J. Chem. Theory Comput*. 1 (2005) 337.

[22] W. Chen, J. Song, P. Guo, W. Cao, J. Bian. Exploring a possible way to synthesize novel better antioxidants based on vitamin E: A DFT study. *Bioorganic Med. Chem. Lett*. 16 (2006) 5874.

[23] J. S. Wright, D. J. Carpenter, D. J. McKay, K. U. Ingold. Theoretical Calculation of Substituent Effects on the O–H Bond Strength of Phenolic Antioxidants Related to Vitamin E. *J. Am. Chem. Soc.* 119 (1997) 4245.

[24] C. Lee, W. Yang, R. G. Parr. Development of the Colle-Salvetti correlation-energy formula into a functional of the electron density. *Phys. Rev. B* 37 (1988) 785.

[25] A. D. Becke. Density-functional thermochemistry. III. The role of exact exchange. *J. Chem. Phys.* 98 (1993) 5648.

[26] S. Grimme, S. Ehrlich, L. Goerigk. Effect of the damping function in dispersion corrected density functional theory. *J. Comput. Chem*. 32 (2011) 1456.

[27] S. Grimme. Density functional theory with London dispersion corrections. *WIREs Comput. Mol. Sci.* 1 (2011) 211.

[28] A. D. Becke, E. R. Johnson. A density-functional model of the dispersion interaction. *J. Chem. Phys*. 123 (2005) 154101.

[29] M. Cossi, N. Rega, G. Scalmani, V. Barone. Energies, structures, and electronic properties of molecules in solution with the C-PCM solvation model. *J. Comput. Chem.* 24 (2003) 669.

[30] C. Gonzalez, H. B. Schlegel. An improved algorithm for reaction path following. *J. Chem. Phys.* 90 (1989) 2154.

[31] S. Kozuch, J. M. L. Martin. DSD-PBEP86: in search of the best double-hybrid DFT with spin-component scaled MP2 and dispersion corrections. *Phys. Chem. Chem. Phys*. 13 (2011) 20104.

[32] L. Goerigk, S. Grimme. Double-hybrid density functionals. *WIRES Comput. Mol. Sci.* 4 (2014) 576.

[33] A. Karton, R. J. O'Reilly, L. Radom. Assessment of theoretical procedures for calculating barrier heights for a diverse set of water-catalyzed proton-transfer reactions. *J. Phys. Chem. A.* 116 (2012) 4211.

[34] A. Karton, L. Goerigk. Accurate reaction barrier heights of pericyclic reactions: Surprisingly large deviations for the CBS-QB3 composite method and their consequences in DFT benchmark studies. *J. Comput. Chem.* 36 (2015) 622.

[35] L.-J Yu, F. Sarrami, R. J. O'Reilly, A. Karton. Reaction barrier heights for cycloreversion of heterocyclic rings: An Achilles' heel for DFT and standard ab initio procedures. *Chem. Phys.* 458 (2015) 1.

[36] L.-J. Yu, F. Sarrami, R. J. O'Reilly, A. Karton. Can DFT and ab initio methods describe all aspects of the potential energy surface of cycloreversion reactions? *Mol. Phys.* 114 (2016) 21.

[37] F. Weigend, R. Ahlrichs. Balanced basis sets of split valence, triple zeta valence and quadruple zeta valence quality for H to Rn: Design and assessment of accuracy. *Phys. Chem. Chem. Phys.* 7 (2005) 3297.

[38] Y. Takano, K. N. Houk. Benchmarking the Conductor-like Polarizable Continuum Model (CPCM) for Aqueous Solvation Free Energies of Neutral and Ionic Organic Molecules. *J. Chem. Theory Comput.* 1 (2005) 70.

[39] Gaussian 16, Revision A.03, M. J. Frisch, G. W. Trucks, H. B. Schlegel, G. E. Scuseria, M. A. Robb, J. R. Cheeseman, G. Scalmani, V. Barone, G. A. Petersson, H. Nakatsuji, X. Li, M. Caricato, A. V. Marenich, J. Bloino, B. G. Janesko, R. Gomperts, B. Mennucci, H. P. Hratchian, J. V. Ortiz, A. F. Izmaylov, J. L. Sonnenberg, D. Williams-Young, F. Ding, F. Lipparini, F. Egidi, J. Goings, B. Peng, A. Petrone, T. Henderson, D. Ranasinghe, V. G. Zakrzewski, J. Gao, N. Rega, G. Zheng, W. Liang, M. Hada, M. Ehara, K. Toyota, R. Fukuda, J. Hasegawa, M. Ishida, T. Nakajima, Y. Honda, O. Kitao, H. Nakai, T. Vreven, K. Throssell, J. A. Montgomery, Jr., J. E. Peralta, F. Ogliaro, M. J. Bearpark, J. J. Heyd, E. N. Brothers, K. N. Kudin, V. N. Staroverov, T. A. Keith, R. Kobayashi, J. Normand, K. Raghavachari, A. P. Rendell, J. C. Burant, S. S. Iyengar, J. Tomasi, M. Cossi, J. M. Millam, M. Klene, C. Adamo, R. Cammi, J. W. Ochterski, R. L. Martin, K. Morokuma, O. Farkas, J. B. Foresman, and D. J. Fox, Gaussian, Inc., Wallingford CT, 2016.

[40] A. A. Kroeger, A. Karton. A Computational Investigation of the Uncatalysed and Water-Catalysed Acyl Rearrangements in Ingenol Esters. *Aust. J. Chem*. 71 (2018) 212.

[41] W. Wan, L.-J. Yu, A. Karton. Mechanistic Insights into Water-Catalyzed Formation of Levoglucosenone from Anhydrosugar Intermediates by Means of High-Level Theoretical Procedures. *Aust. J. Chem*. 69 (2016) 943.

[42] A. Karton. Inorganic acid-catalyzed tautomerization of vinyl alcohol to acetaldehyde. *Chem. Phys. Lett*. 592 (2014) 330.

[43] F. Sarrami, L.-J. Yu, W. Wan, A. Karton. Sulphuric acid-catalysed formation of hemiacetal from glyoxal and ethanol. *Chem. Phys. Lett*. 675 (2017) 27.

[44] L. Vereecken, J. S. Francisco. Theoretical studies of atmospheric reaction mechanisms in the troposphere. *Chem. Soc. Rev.* 41 (2012) 6259.

[45] E. Vöhringer-Martinez, B. Hansmann, H. Hernandez, J. S. Francisco, J. Troe, B. Abel. Water catalysis of a radical-molecule gas-phase reaction. *Science* 315 (2007) 497.

[46] G. da Silva. Carboxylic acid catalyzed keto-enol tautomerizations in the gas phase. *Angew. Chem. Int. Ed.* 49 (2010) 7523.

[47] H. B. Bürgi, J. D. Dunitz, E. Shefter. Geometrical reaction coordinates. II. Nucleophilic addition to a carbonyl group. *J. Am. Chem. Soc.* 95 (1973) 5065.

[48] G. W. Burton, T. Doba, E. Gabe, L. Hughes, F. L. Lee, L. Prasad, K. U. Ingold. Autoxidation of biological molecules. 4. Maximizing the antioxidant activity of phenols. *J. Am. Chem. Soc*. 107 (1985) 7053.

[49] K. Mukai, K. Daifuku, K. Okabe, T. Tanigaki, K. Inoue. Structure-activity relationship in the quenching reaction of singlet oxygen by tocopherol (vitamin E) derivatives and related phenols. Finding of linear correlation between the rates of quenching of singlet oxygen and scavenging of peroxyl and phenoxyl radicals in solution. *J. Org. Chem.* 56 (1991) 4188.

[50] S. Gutiérrez-Oliva. Theoretical study of the hydrogen abstraction from vitamin-E analogues. The usefulness of DFT descriptors. *J. Mol. Model*. 17 (2011) 593.